Relationship between structure and mechanical properties in high-modulus poly(2,5(6)-benzoxazole) (ABPBO) fibres

R. J. Young* and P. P. Ang
Polymer Science and Technology Group, Manchester Materials Science Centre, UMIST and University of Manchester, Manchester M60 1QD, UK
(Received 16 November 1990; revised 14 December 1990; accepted 14 December 1990)

The relationship between structure and mechanical properties has been investigated for high-modulus fibres of poly(2,5(6)-benzoxazole) (ABPBO). It has been found that the modulus of the fibres increases from 91 to 133 GPa upon heat treatment at 525°C. The strain to failure decreases from about 4.3% to 2.0%, whereas the fibre strength remains virtually unchanged at about 2.1 GPa. The improvement in fibre modulus is accompanied by the development of a three-dimensional crystal order in the fibres. Molecular deformation in the fibres has been monitored using Raman microscopy and it has been shown that the position of the Raman bands in the fibres is sensitive to the application of mechanical stress. This has enabled a detailed study of molecular deformation in the fibres to be undertaken for both tensile and compressive deformation. It has been found that failure takes place at relatively low stresses and strains in compression through the formation of kink bands. It has also been shown that the fibres tend to have a lower modulus in compression than for tensile deformation. The molecular processes involved during fibre deformation have been discussed in detail.

(Keywords: high-modulus fibres; Raman spectroscopy; mechanical properties; compressive behaviour)

INTRODUCTION

There is currently considerable interest in preparing polymer fibres with high levels of stiffness and strength for applications such as fibre-reinforced polymers. This present paper is concerned with the relationship between structure and mechanical properties of fibres of the stiff-chain molecule poly(2,5(6)-benzoxazole) (ABPBO). This material has been produced under the US Air Force ordered polymer programme, and the fibres are reported to have excellent mechanical properties[1-3]. Rigid-rod polymer fibres produced under the same programme, i.e. poly(*p*-phenylene benzobisthiazole) (PBT)[4] and poly(*p*-phenylene benzobisoxazole) (PBO)[5], are also found to have impressive properties.

This present study reports the results of part of a large programme in the Manchester Materials Science Centre concerned with the analysis of the deformation of fibres and composites using Raman microscopy. It has been found that molecular deformation can be followed by Raman microscopy in a wide variety of high-performance fibres such as PBT[4], PBO[5], aromatic polyamides[6] and carbon[7]. As well as analysing molecular deformation in free-standing fibres, it is also possible to use the Raman technique to follow fibre deformation within composites[8]. The technique is also applicable to ceramic fibres such as Nicalon[9] and some isotropic polymers such as specially synthesized urethane–diacetylene segmented block copolymers[10].

In this present investigation the structure of both as-spun and heat-treated ABPBO fibres has been examined by electron microscopy, and their mechanical behaviour, in particular Young's modulus and ultimate properties, has been determined. Raman microscopy[4,5] has been used to follow molecular deformation in the fibres during both elastic and plastic deformation. By embedding individual fibres in an epoxy resin it has been possible to follow molecular deformation during axial compression of the fibres and to follow the onset of compressive failure through the formation of kink bands. The behaviour of the ABPBO fibres will be compared with that of other high-performance fibres.

* To whom correspondence should be addressed

EXPERIMENTAL

Materials and characterization

The ABPBO fibres used in this study were supplied by the Materials Laboratory, Wright-Patterson Air Force Base, Ohio, USA, and were based on the molecule poly(2,5(6)-benzoxazole) (ABPBO):

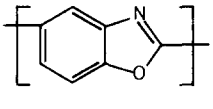

Two types of fibres were supplied and both were about 16 μm in diameter: first, straw-coloured 'as-spun' (AS) fibres prepared from a concentrated acid solution of the polymer; second, higher-modulus darker fibres, which had been heat treated (HT) at 525°C under tension.

The structure and perfection of individual fibres was evaluated using a scanning electron microscope (Philips 505 operated at 10 kV). The fibres were cleaned with a

0032-3861/92/050975-08

solvent and rendered conductive by sputter coating within a thin layer of gold. The fibres were also examined optically to determine their diameter using an Olympus Manager optical microscope system with a $\times 40$ objective.

Wide-angle X-ray scattering (WAXS) patterns were obtained from bundles of the two types of fibres using a flat-plate transmission geometry in nickel-filtered Cu Kα radiation. This enabled the degree of perfection and the level of molecular orientation in the different fibres to be compared.

Mechanical testing

Individual ABPBO fibres were mounted across holes on paper cards using a slow-setting, cold-curing epoxy resin adhesive. Once the adhesive had set the pieces of card were mounted between fibre testing grips in a model 1121 Instron mechanical testing machine and the card edges were cut. Data for stress–strain curves were collected using an HP85 computer and also on chart paper. Load ranges of between 2 and 5 N were employed using a 5 N capacity load cell. A variety of gauge lengths ranging from 50 to 130 mm were employed and the strain was determined from the crosshead displacement. A crosshead speed of 1 mm min^{-1} was employed in all cases, making an initial strain rate ranging from 3.3×10^{-4} to 1.3×10^{-4} s^{-1} depending upon the gauge length. At least 10 samples of each type of fibre were employed. All tests were carried out at 23 ± 1°C and 50 ± 5% relative humidity.

Single-fibre composite specimens

Two types of single-fibre composite specimens were prepared consisting of individual ABPBO fibres in Ciba-Geigy XD1927 two-part solvent-free cold-setting epoxy resin matrix. The first type consisted of a 5 mm thick dog-bone shaped resin tensile bar (gauge length 30 mm) with a single filament of ABPBO aligned within the resin along the length of the bar. This was used for monitoring the tensile deformation of continuous embedded fibres. The second type was a rectangular block (5 mm $\times$ 6 mm $\times$ 12 mm) of the same resin cut from the tensile bars and was used for evaluating the axial compressive behaviour of the fibres. Resistance strain gauges with a gauge factor of 2.06 were attached along the length of the specimens to measure the level of axial strain. The specimens were deformed in a Polymer Laboratories 'Mini-Mat' Materials tester in both the Raman microscope system and a standard optical microscope at room temperature, 22 ± 2°C.

Raman microscopy

Raman spectra were obtained from both free-standing fibres in air and from fibres embedded in the epoxy resin specimens, using a Raman microscope system. This is based upon a SPEX 1403 double monochromator connected to a modified Nikon optical microscope. Spectra were obtained at a resolution of the order of ± 5 cm^{-1} using the 632.8 nm line of a 10 mW He–Ne laser for the AS ABPBO fibres. Because of problems with fluorescence the 488 nm line of an argon-ion laser operated at about 10 mW was also employed for the HT fibres. A $\times 40$ objective lens with a numerical aperture of 0.65 was used for the study of free-standing fibres, and this gave a spot size of 2 μm when focused. In the case of the embedded fibres a larger spot size was employed using a $\times 20$ objective lens of numerical aperture 0.40. The spectra were recorded using a liquid N_2 cooled Wright Instruments CCD system, which has very low noise and enables the rapid determination of spectra in typically of the order of 10 s for one Raman peak in ABPBO.

Free-standing fibres were deformed in the Raman microscope at room temperature using an aluminium deformation stage driven by a hand-operated micrometer. Fibres were fixed to the stage using a cyanoacrylate adhesive and aluminium foil tabs. A gauge length of about 20 mm was employed and the strain was determined from the micrometer displacement.

RESULTS AND DISCUSSION

Fibre structure

The structureof ABPBO fibres has been examined in detail by Adams and coworkers[1–3] and so it will only be discussed briefly. WAXS patterns for the AS ABPBO and the HT ABPBO fibres are shown in *Figures 1a* and *1b*, respectively, and it can be seen that there is a dramatic change in structural organization during the heat treatment. In the case of the AS fibre (*Figure 1a*) there are only two pairs of equatorial reflections and there is considerable diffuse scattering. The WAXS pattern for the HT fibre (*Figure 1b*) is more well defined and shows strong equatorial reflections, better molecular orientation, several meridional reflections and a number of off-axis

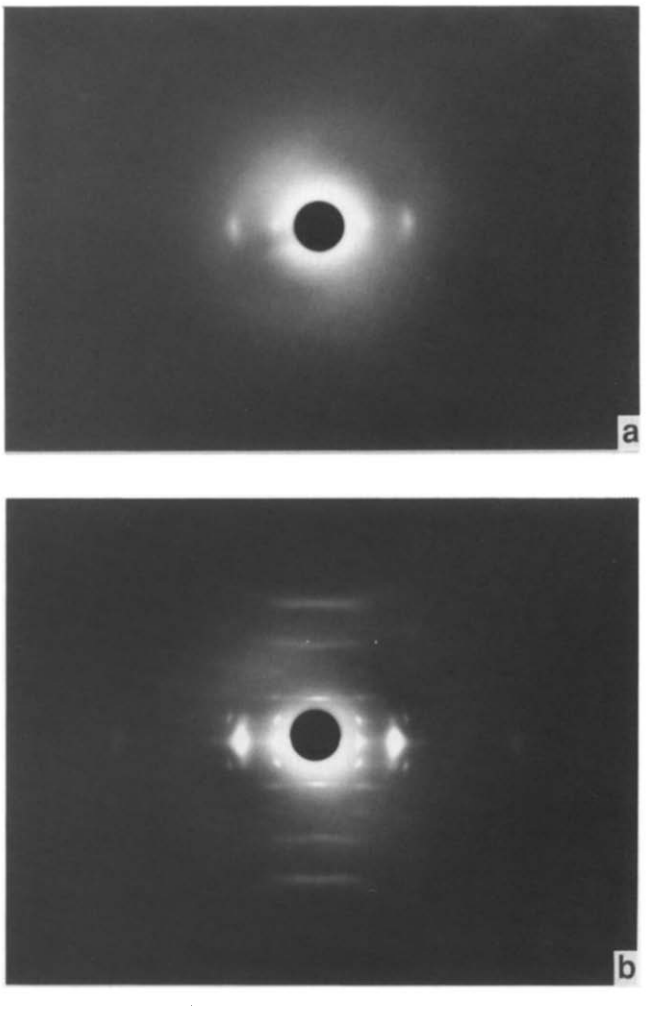

Figure 1 Wide-angle X-ray diffraction patterns obtained from (a) AS ABPBO and (b) HT ABPBO fibres

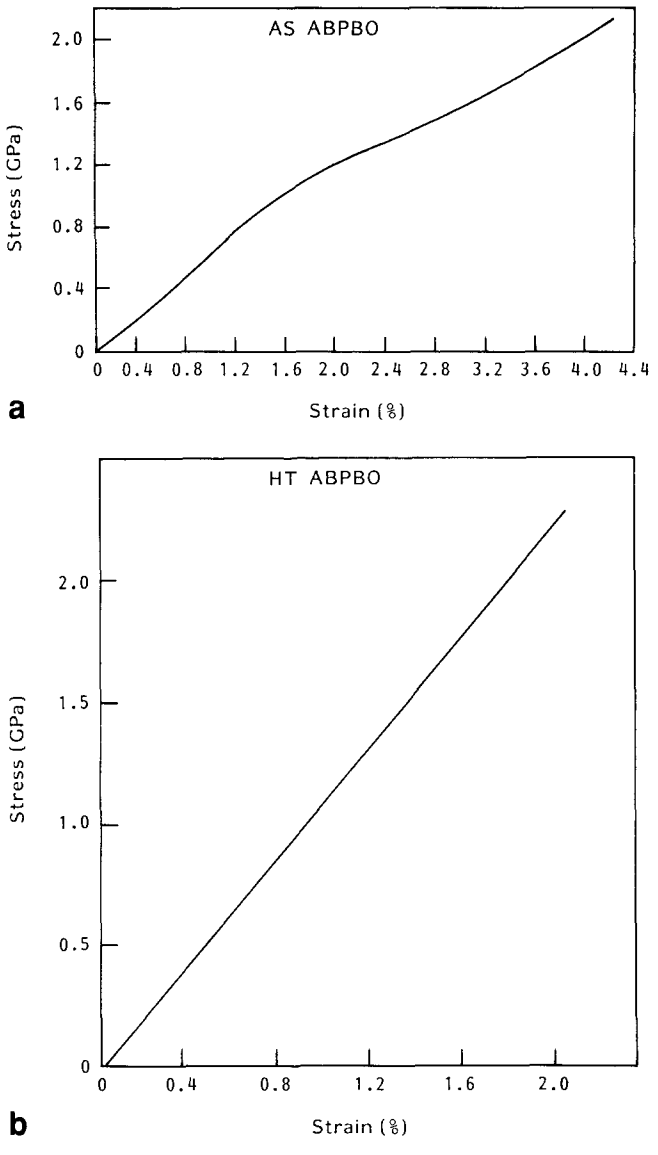

Figure 2 Stress–strain curves for individual fibres of (a) AS ABPBO and (b) HT ABPBO

(*hkl*) reflections. These findings are similar to those of Adams and coworkers[1] and show that ABPBO has a fairly well defined three-dimensional (3D) crystalline structure. This should be contrasted with PBT[4] where there is considerable axial disorder in the structure resulting in the absence of off-axis (*hkl*) reflections. Fibres of PBO[5] have rather better chain axis registry but the 3D crystal structure of ABPBO is considerably better defined than that of the rigid-rod polymers and bears more similarity to that of aromatic polyamides such as poly(*p*-phenylene terephthalamide) (e.g. Kevlar[11]). Adams and coworkers[1] suggested that this may be because ABPBO is not a true rigid-rod polymer but is a stiff-chain molecule in an extended planar zig-zag conformation, as in the case of poly(*p*-phenylene terephthalamide).

Mechanical testing

Stress–strain curves obtained from individual fibres of AS and HT ABPBO are shown in *Figures 2a* and *2b*, respectively. It can be seen that for the AS fibre there is a pronounced 'knee' in the stress–strain curve corresponding to yield at a strain of about 1.3%. In contrast the stress–strain curve for the HT fibre (*Figure 2b*) shows approximately linear behaviour up to fracture at about 2% strain. It can be seen that there is also an increase in the slope of the stress–strain curve of the fibres following heat treatment, showing that the HT fibres have a significantly higher value of Young's modulus.

The values of Young's modulus and fracture properties for individual high-performance fibres depend upon gauge length. The measured Young's modulus (E) tends to increase with increasing gauge length due to the elimination of end effects, whereas the strength (σ_f) and elongation to failure (e_f) both tend to decrease with increasing gauge length due to the increasing likelihood of finding defects in the fibre. In order to obtain geometry-independent values of E, σ_f and e_f, measurements were made at four different gauge lengths. The E data were then extrapolated to infinite gauge length and the data for σ_f and e_f extrapolated to zero gauge length. The extrapolated values of E, σ_f and e_f are presented in *Table 1*. It can be seen that the heat treatment causes the modulus of ABPBO fibres to increase from 91 to 133 GPa and e_f to decrease from about 4.3% to 2.0% while the value of σ_f remains approximately unchanged at about 2.1 GPa.

Molecular deformation

The molecular deformation of the AS and HT ABPBO fibres was investigated using Raman microscopy. A Raman spectrum in the region 1100–1700 cm^{-1} is given in *Figure 3* for an AS ABPBO fibre. It can be seen that there are over 10 well defined Raman bands in the spectrum. The Raman spectrum for the HT ABPBO fibre is by no means so well defined and consists of only a few peaks on a strong fluorescent background. The increase in fluorescence during the heat treatment at 525°C may

Table 1 Extrapolated values of Young's modulus (E), tensile strength (σ_f) and elongation to failure (e_f) for the ABPBO fibres

Fibre	E (GPa)	σ_f (GPa)	e_f (%)
AS ABPBO	91 ± 5	2.1 ± 0.3	4.3 ± 0.5
HT ABPBO	133 ± 11	2.2 ± 0.3	2.0 ± 0.3

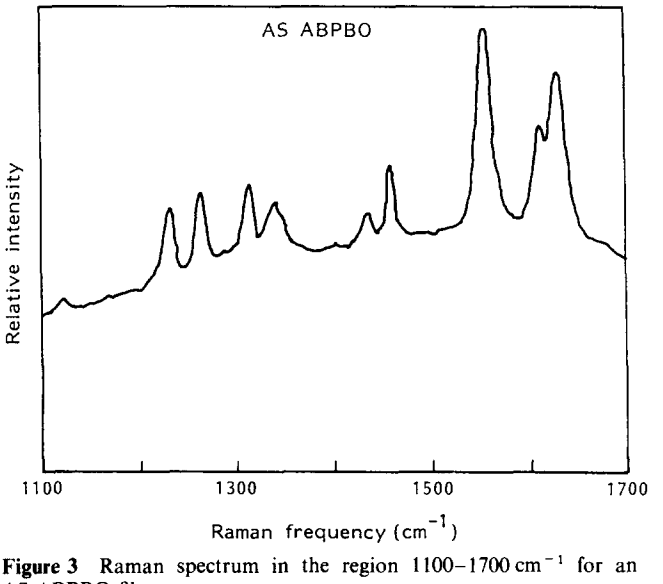

Figure 3 Raman spectrum in the region 1100–1700 cm^{-1} for an AS ABPBO fibre

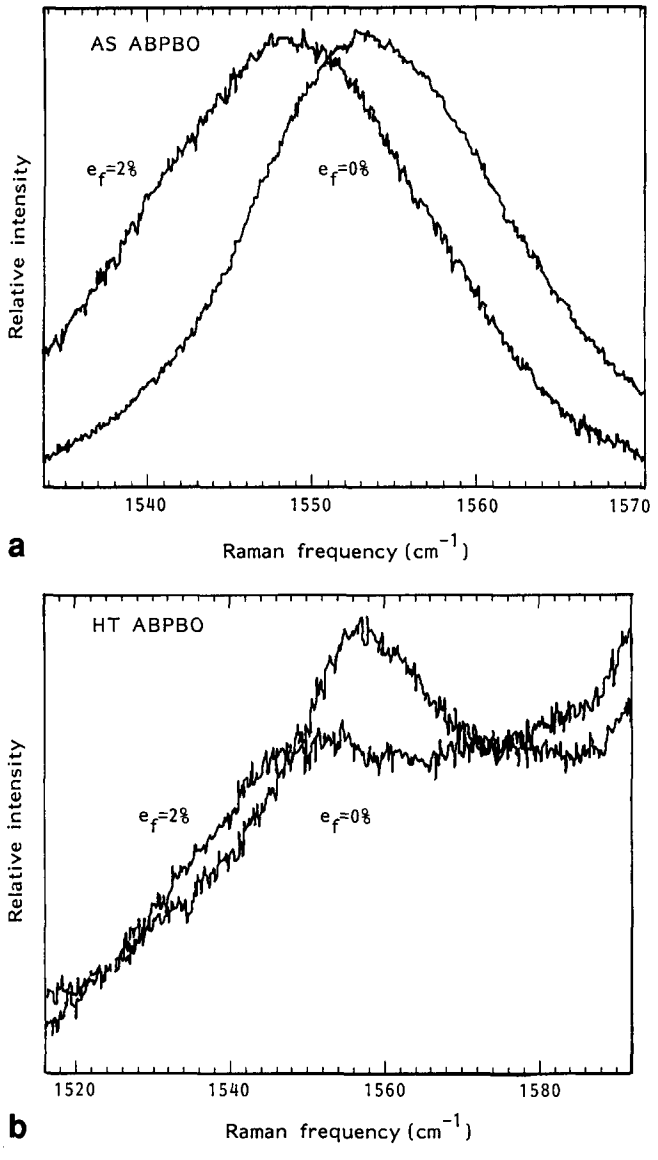

Figure 4 Raman spectra in the region of 1555 cm^{-1} before and after tensile deformation to 2% strain for (a) AS ABPBO and (b) HT ABPBO fibres

be a result of thermal degradation of the fibres taking place.

It was found that the peak positions for the different Raman bands in both types of fibres were sensitive to the application of stress or strain and tended to shift, normally to lower frequency, when the fibres were deformed. Most of the present investigation has concentrated upon the strong Raman band at about 1550–1560 cm^{-1}, and the effect of deformation upon the band is shown in *Figure 4* for both AS and HT ABPBO. It can be seen that in both cases the peak position shifts to lower frequency and tends to broaden. It can also be seen that the band in HT ABPBO (*Figure 4b*) is considerably less well defined due to the strong fluorescent background. The shift in peak position is a direct indication of the effect of the application of macroscopic stress to the fibre causing molecular main-chain deformation leading to a change in the bond-stretching force constants. The broadening is an indication that there is a range of molecular stress and strain within the fibres.

The variation in peak position for the 1550–1560 cm^{-1} band with fibre strain is shown in *Figure 5* for the two types of ABPBO fibre. In *Figure 5a* data are given for four separate experiments on different samples of the AS ABPBO fibres to show the reproducibility of the measurements. It can be seen that there is an approximately linear shift in peak position with applied strain up to about 1.3% at which point there is no further shift in peak position. This corresponds to the strain for the onset of yielding as found from the stress–strain measurements (*Figure 2a*). It shows that up to the yield strain the molecules in the fibres are undergoing chain stretching but after yield there is no further stretching and deformation probably proceeds by the molecules sliding past each other. It can also be seen from *Figure 5a* that the data are reproducible to about ± 1 cm^{-1}. This is due to a combination of fibre-to-fibre variation within the batch tested and difficulties in deciding the zero-strain position for the fibres.

The variation in peak position for the HT ABPBO fibre as a function of fibre strain is shown in *Figure 5b*. It can be seen that there is an approximately linear shift in the peak position up to failure. This is entirely consistent with the stress–strain behaviour of HT ABPBO (*Figure 2b*) where the stress–strain curve is approximately linear up to failure. Hence it appears that the improvement in molecular ordering following heat treatment inhibits molecular sliding and deformation in HT ABPBO takes place principally by chain stretching. The shift in the elastic region for AS ABPBO is about 3.9 ± 0.2 cm^{-1}/% strain and about 5.9 ± 0.3 cm^{-1}/% strain for HT ABPBO. If the rate of shift is $d\Delta\nu/de$ where

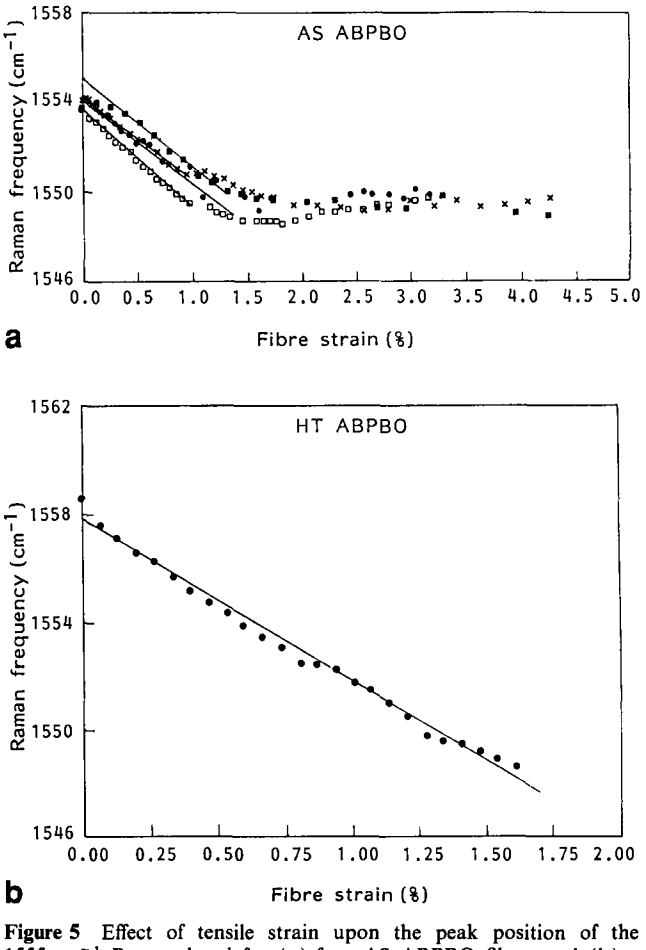

Figure 5 Effect of tensile strain upon the peak position of the 1555 cm^{-1} Raman band for (a) four AS ABPBO fibres and (b) a HT ABPBO fibre

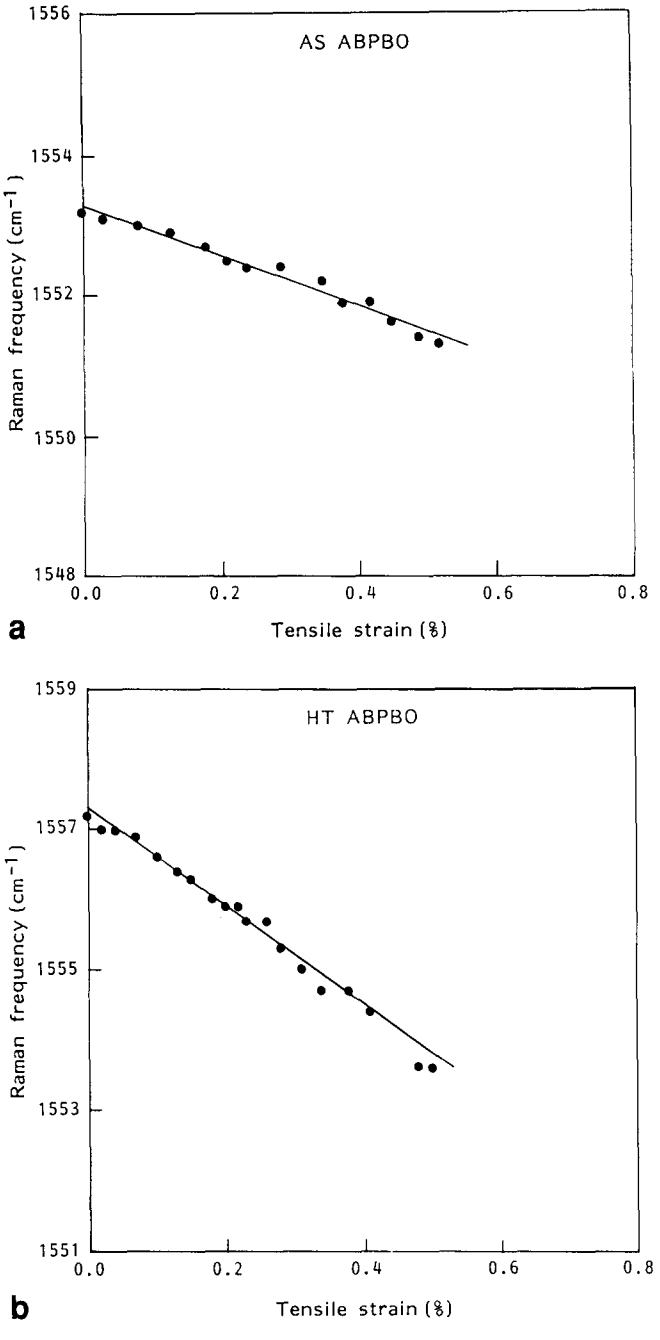

Figure 6 Effect of tensile strain upon the peak position of the 1555 cm^{-1} Raman band for embedded fibres of (a) AS ABPBO and (b) HT ABPBO

$\Delta\nu$ is the Raman frequency and e is the strain, then:

$$\frac{d\Delta\nu/de(HT)}{d\Delta\nu/de(AS)} = \frac{5.9}{3.9} = 1.51$$

The ratio of the modulus for the two types of fibre is given by:

$$\frac{E(HT)}{E(AS)} = \frac{133}{91} = 1.46$$

Since these two ratios are virtually identical it means that $d\Delta\nu/de$ is approximately proportional to E as is found for other high-modulus fibres[4,6]. Hence $d\Delta\nu/d\sigma$ will be the same for both types of fibres, and the analysis shows that the Raman technique is directly monitoring the *molecular stress* of the fibres rather than molecular strain. The improved ordering in the HT fibre means that the macroscopic deformation is transferred more efficiently to the molecules within the fibres and hence they have a higher value of Young's modulus. It also shows that, since $d\Delta\nu/de$ is proportional to the fibre modulus E, once a material is calibrated for the Raman technique the modulus of a sample can be determined indirectly from $d\Delta\nu/de$.

Fibre compression

It is well known[12] that, although high-modulus polymer fibres can have excellent mechanical properties during tensile deformation, they are prone to failure in compression at relatively low levels of stress and strain and it is probably this problem, more than any other, which limits their wider use in engineering applications. Unfortunately, it is relatively difficult to determine the axial compressive behaviour of individual filaments of 16 μm diameter fibres. Indirect methods such as tensile recoil[13] have been used, but in this present study fibre compression has been followed from the compressive deformation of blocks of epoxy resin containing single ABPBO fibres. This is similar to the method developed by van der Zwaag[14] and coworkers for studying the compressive behavour of aromatic polyamide fibres.

The low-strain tensile behaviour of the fibres within the resin was first monitored using Raman microscopy. The epoxy resin employed is sufficiently free from fluorescence such that good spectra could be obtained from the individual fibres within the resin. The variation of the Raman peak position with tensile strain (monitored using a strain gauge) is shown in *Figure 6* for the single-fibre tensile bars. The behaviour is essentially identical to that of the free-standing fibres in air (*Figure 5*) and similar values of $d\Delta\nu/de$ are obtained. The tensile deformation was maintained below 0.6% strain to avoid either fibre or resin yielding.

Rectangular blocks were cut from the same bars and compressed in the Raman microscope system to an overall strain of about 1%. The variation of Raman peak position with compressive strain is shown in *Figure 7* for both AS and HT ABPBO fibres. It can be seen that the Raman frequency *increases* with strain in compression until a critical value at which point there is no further increase. This corresponds to the strain, e_c, at which compressive failure of the fibres takes place. It is found that failure occurs at about 0.6% strain for the AS ABPBO fibres (*Figure 7a*) and 0.3% for the HT ABPBO fibres (*Figure 7b*). These values are presented in *Table 2*.

The compressive deformation of the fibres was also monitored by transmission optical microscopy as shown in *Figure 8* for an AS ABPBO fibre. A series of micrographs are shown at four indicated strain levels for the same region of a fibre in the epoxy resin block. It can be seen that, as the strain is increased, kink bands start to form until at the highest level of strain (1.4%) there are kink bands along the entire length of the fibre. It is more difficult to see the kink bands in the HT ABPBO fibres using optical microscopy because the heat treatment causes the fibres to become more opaque. However, careful examination of optical micrographs obtained from HT ABPBO fibres has enabled the onset of kink band formation to be observed.

Figure 9 shows the dependence of the number of kink bands along a given length of fibre (1 mm) upon compressive strain for both AS and HT ABPBO fibres. There are a few pre-existing kink bands in the fibres

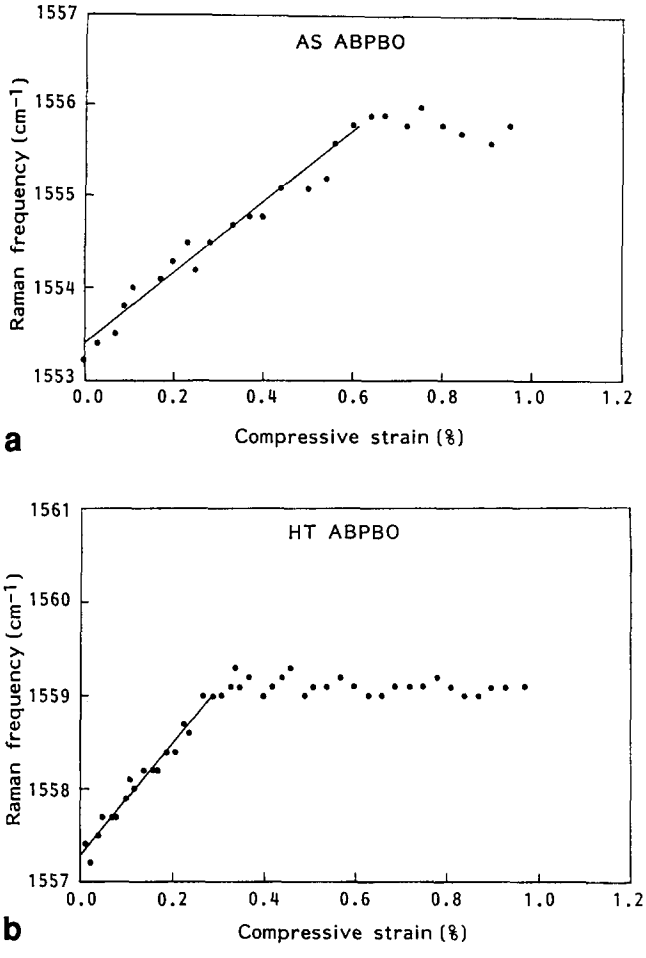

Figure 7 Effect of compressive strain upon the peak position of the 1555 cm^{-1} Raman band for embedded fibres of (a) AS ABPBO and (b) HT ABPBO

Table 2 Values of compressive failure strain (e_c) determined from Raman microscopy and critical strain for kink band formation (e_k) determined by direct observations. The corresponding critical stresses σ_c and σ_k are also shown

Fibre	e_c (%)	e_k (%)	σ_c (GPa)	σ_k (GPa)
AS ABPBO	0.60	0.87	0.49	0.71
HT ABPBO	0.27	0.38	0.32	0.46

before compressive deformation which either were caused by the manufacturing process or were formed during handling. This number remains constant until a critical value of strain at which point there is a rapid increase in the number of kink bands. This corresponds to the critical strain for kink band formation, e_k, and is about 0.8% for the AS fibre and 0.4% for the HT fibre (*Table 2*). It appears that the value of e_c obtained by the Raman technique is lower than e_k obtained by direct observation (*Table 2*). This is not surprising since the Raman method probes molecular deformation processes and can monitor the changes in molecular stressing which occur as a precursor to visual kink band formation.

Since it was shown earlier that the strain-induced Raman frequency shift is essentially a measure of molecular stress, it follows that the data contained in *Figures 6* and *7* allow full 'molecular' stress–strain curves to be constructed for both tensile and compressive deformation. These are shown in *Figure 10* where the frequency shift is plotted as a function of strain for the AS and HT ABPBO fibres using the data from *Figures 6* and *7*. The full curves are fits of the data points to third-order polynomials, and it can be seen that there is a gradual decrease in the slope of the line on going from tension through zero strain into compression. Hence the fibres behave in a nonlinear elastic manner. The failure of the fibres through the onset of kink band formation causes an abrupt change in slope of the line at e_c as described earlier.

Similar tensile/compressive data for other high-modulus fibres have been presented by Galiotis and coworkers[15] as two straight lines in the elastic region with an abrupt change in slope at zero strain. However, from considerations of both molecular and macroscopic mechanics, such behaviour is impossible since there cannot be a step change slope at the origin. Indeed, inspection of their data shows that they can also be fitted to a continuous curve for their high-modulus fibres[15].

The data in *Figure 10* show that, for both AS and HT ABPBO fibres, the Young's modulus of the fibres decreases on going from tension into compression since $d\Delta\nu/de \propto E$. The ratios of the compressive to tensile moduli at different strain levels up to about $\pm 0.5\%$ strain are about 0.9 and are similar for the two types of fibres. There are at least two possible explanations of this

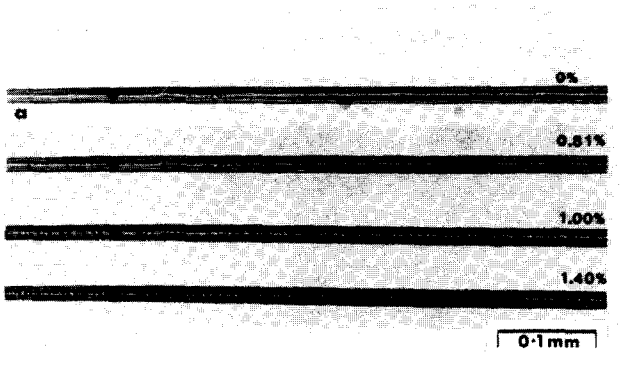

Figure 8 Transmission optical micrographs of the same area of a single AS ABPBO fibre embedded in an epoxy resin and subjected to the different stated level of applied compressive strain

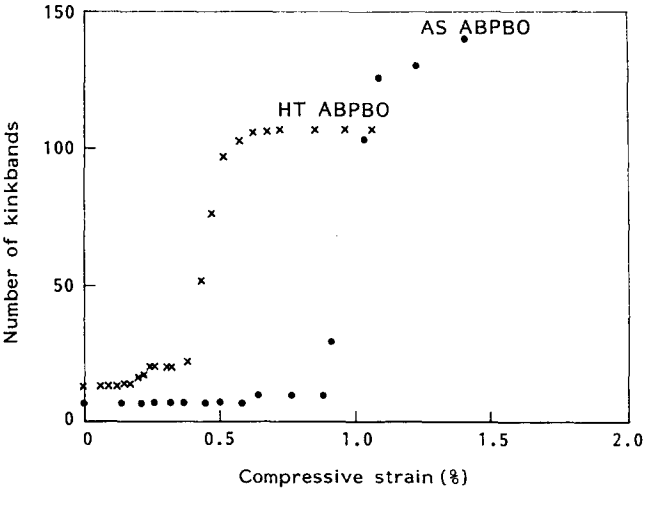

Figure 9 Dependence of the number of kink bands along a fixed length of an embedded fibre upon the level of axial compressive strain for AS ABPBO (●) and HT ABPBO fibres (×)

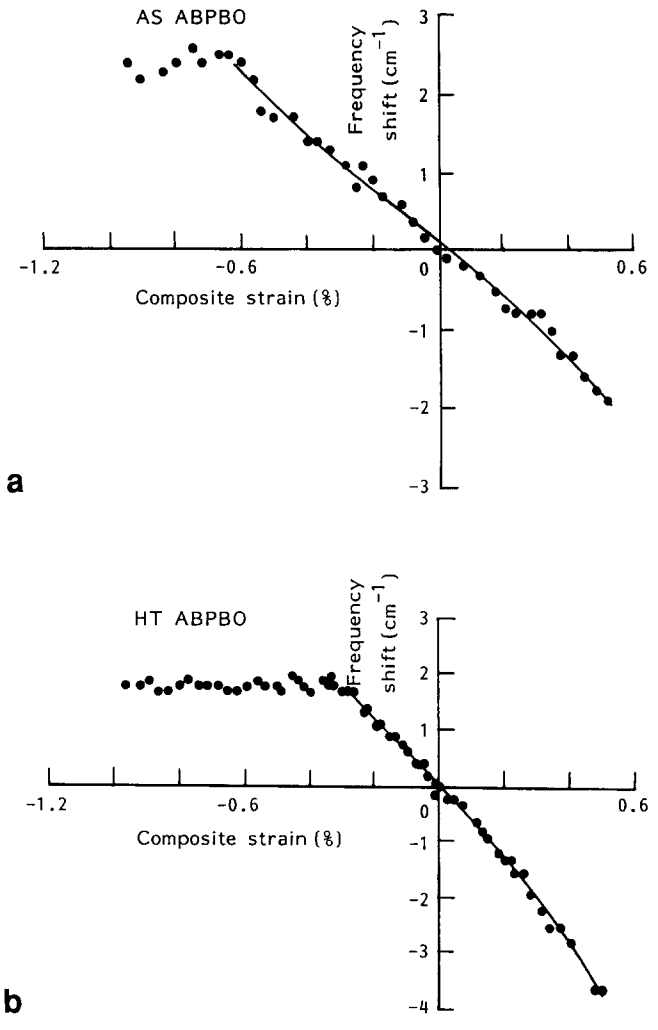

Figure 10 Dependence of peak position for the 1555 cm^{-1} Raman band upon both tensile (positive) and compressive (negative) strain for embedded fibres of (a) AS ABPBO and (b) HT ABPBO. The full curves are fits of the experimental data during elastic deformation to third-order polynomials

variation in modulus. It is possible that it could be due to microstructural factors such as the rotation of crystallites during deformation as has been postulated for aramid fibres[16]. This could lead to stiffening of the fibres during tensile deformation and softening of the fibres in compression. Alternatively it may be caused by an inherent difference in molecular stiffness for the two types of deformation. Indeed, *ab initio* quantum-mechanical calculations by Adams and coworkers[17] of the deformation of rigid-rod molecules have indicated that they are normally significantly less stiff in compression than in tension. Clearly this is an area where more work is needed before the behaviour can be fully understood.

Since the data in *Figure 10* show that the compressive moduli of the fibres are of the order of 90% of the tensile moduli, it is possible to estimate the critical stresses σ_c and σ_k for fibre failure and kink band formation, respectively, from the values of e_c and e_k. They are also given in *Table 2* and it can be seen that even when the modulus difference is taken into account σ_c and σ_k are both higher for the AS ABPBO fibres than for the HT fibres. The ratio of compressive to tensile strength is only of the order of 0.2 for both fibres, showing that, in common with other high-modulus polymer fibres, they are considerably weaker in compression than when deformed in tension. It would seem that this behaviour is an inherent property of high-modulus polymer fibres, although it is a phenomenon that is not yet properly understood. However, before this can be done it is essential that accurate and reliable measurements of fibre compressive properties are required, and it is clear that the results of this study go a long way towards providing such information.

CONCLUSIONS

It has been shown that fibres of ABPBO have impressive mechanical properties. The as-spun fibres have a modulus of about 91 GPa, which increases to 133 GPa following heat treatment at 525°C. Since the fibre strength remains constant at 2.1 GPa there is a consequent reduction in elongation to break from 4.3% to about 2%. The increase in modulus is accompanied by an improvement in the crystallographic order in the fibres. Deformation has been followed using Raman microscopy and it has been shown that the position of the Raman bands is sensitive to the application of mechanical stress. It has been demonstrated that the dependence of the frequency of the 1555 cm^{-1} Raman band upon strain $d\Delta\nu/de$ is proportional to the fibre modulus, indicating that the technique is a measure of fibre stress rather than fibre strain. This information has been used to show that by using a combination of tensile and compressive deformation of embedded fibres the fibres have a lower modulus in compression than in tension. The onset of fibre failure in compression has been monitored by a combination of Raman microscopy and the direct observation of kink band formation. It has been found that the fibres undergo compressive yielding at lower stresses and strains than are required for the formation of large numbers of kink bands. It has also been demonstrated that the higher-modulus heat-treated fibres have inferior compressive properties than the lower-modulus as-spun fibres. It is therefore shown that the combination of mechanical deformation and Raman microscopy is a powerful method of evaluating the mechanical behaviour of high-performance fibres.

ACKNOWLEDGEMENTS

The authors are grateful to Dr R. J. Day (UMIST) and Dr W. W. Adams (USAF) for valuable discussions. The work was supported by research grants from the USAF European Research Office and the SERC.

REFERENCES

1 Krause, S. J., Haddock, T. B., Vezie, D. L., Lenhert, P. G., Hwang, W.-F., Price, G. E., Helminiak, T. E., O'Brien, J. F. and Adams, W. W. *Polymer* 1988, **29**, 1354
2 Fatimi, A. V., Cross, E. M., O'Brien, J. F. and Adams, W. W. *J. Macromol. Sci.–Phys. (B)* 1986, **24**, 159
3 Krause, S. J., Haddock, T. and Adams, W. W. Proc. 42nd Annual Meeting of the Electron Microscopy Society of America, 1984, p. 382
4 Day, R. J., Robinson, I. M., Zakikhani, M. and Young, R. J. *Polymer* 1987, **28**, 1833
5 Young, R. J., Day, R. J. and Zakikhani, M. *J. Mater. Sci.* 1990, **25**, 127
6 Young, R. J., Lu, D. and Day, R. J. *Polym. Int.* 1991, **24**, 71
7 Robinson, I. M., Zakikhani, M., Day, R. J., Young, R. J. and Galiotis, C. *J. Mater. Sci. Lett.* 1987, **6**, 1212

8 Young, R. J., Galiotis, C., Robinson, I. M. and Batchelder, D. N. *J. Mater. Sci.* 1987, **22**, 3642
9 Day, R. J., Piddock, V., Taylor, R., Young, R. J. and Zakikhani, M. *J. Mater. Sci.* 1989, **24**, 2898
10 Stanford, J. L., Young, R. J. and Day, R. J. *Polymer* 1991, **32**, 1713
11 Northolt, M. G. and van Aartsen, J. *J. Polym. Sci., Polym. Symp.* 1977, **58**, 283
12 DeTeresa, S. J., Porter, R. S. and Farris, R. J. *J. Mater. Sci.* 1985, **20**, 1645
13 Allen, S. R. *J. Mater. Sci.* 1987, **22**, 853
14 van der Zwaag, S., Picken, S. J. and van Sluijs, C. P., in 'Integration of Fundamental Polymer Science and Technology' (Eds. P. J. Lemstra and L. A. Kleintjens), Elsevier Applied Science, London, Vol. 3, p. 199
15 Galiotis, C. and Vlattas, C. *Polymer* 1991, **32**, 1788
16 van der Zwaag, S., Northolt, M. G., Young, R. J., Galiotis, C., Robinson, I. M. and Batchelder, D. N. *Polym. Commun.* 1987, **28**, 276
17 Adams, W. W., Dudis, D. S., Wierschke, S. G. and Shoemaker, J. R., USAF, personal communication